Neurochemistry International 81 (2015) 48–56

Contents lists available at ScienceDirect

Neurochemistry International

journal homepage: www.elsevier.com/locate/nci

Acetylation and phosphorylation of STAT3 are involved in the responsiveness of microglia to beta amyloid

Margherita Eufemi [a,1], Rossana Cocchiola [a,1], Donatella Romaniello [a], Virginia Correani [a], Laura Di Francesco [a], Cinzia Fabrizi [b], Bruno Maras [a], M. Eugenia Schininà [a,*]

[a] Dipartimento di Scienze Biochimiche, Sapienza, University of Rome, P.le Aldo Moro, 5 00185 Rome, Italy
[b] Dipartimento di Scienze Anatomiche, Istologiche, Medico-Legali e dell'Apparato Locomotore, Sapienza, University of Rome, Via Borelli, 50 00161 Rome, Italy

ARTICLE INFO

Article history:
Received 6 June 2014
Received in revised form 15 January 2015
Accepted 20 January 2015
Available online 26 January 2015

Keywords:
STAT3
14-3-3epsilon
Alzheimer's disease
Amyloid beta peptides
Microglia

ABSTRACT

Microglia are macrophages within the central nervous system playing a central role in neurodegenerative disorders. Although the initial engagement of microglia seems to be neuroprotective, many lines of evidence indicate that its persistent activation contributes to dismantle neuronal activity and to induce neuronal loss. The molecular pathways that lead from amyloid interaction with membrane receptors to the microglial activation have been extensively investigated, although a definitive picture is not yet at hand. In this work, primary and immortalized microglial cells were treated with a synthetic form of Aβ peptides, and relative abundance of acetylated and phosphorylated STAT3 were assayed. Results highlight, for the first time, three distinctive sequential events: i) an earlier event marked by the increase in the level of STAT3 acetylated species, followed by ii) a later increase in the level of STAT3 phosphorylated form, and finally iii) an involvement of phosphorylated STAT3 in the increase in expression of the 14-3-3 epsilon, a protein frequently associated with neurodegenerative diseases and known to be a marker of Aβ-activated microglia. These data outline a complex, time-dependent modification of STAT3 signalling triggered by amyloid in the microglial compartments, that once confirmed by *in vivo* experiments will broaden the knowledge of the molecular basis of amyloid neurotoxicity.

1. Introduction

Microglia-mediated inflammation in the central nervous system is a hallmark of the pathogenesis of several neurodegenerative diseases including Alzheimer's disease (AD; Solito and Sastre, 2012; Cunningham, 2013; Prokop et al., 2013; Birch et al., 2014). In the healthy tissue, microglia cooperate with astrocytes, a component of the glial compartment with an eminent trophic function in maintaining the balance between production and clearance of amyloid beta peptides $A\beta_{1-40}$ and $A\beta_{1-42}$ released by the sequential cleavage of the membrane Amyloid Precursor Protein (APP) by beta and gamma secretases (Blennow et al., 2006; Herber et al., 2007; Thal, 2012). When this equilibrium is broken as in AD, production of Aβ peptides overcomes their removal, and toxic oligomeric species may arise, and thus damage neurones, glial cells and synapses (Ballard et al., 2011; Mawuenyega et al., 2010; Morkuniene et al., 2013). In the presence of these toxic species, microglia release pro-inflammatory cytokines such as TNF-alpha, interleukin 6 (IL-6) and interleukin 1 beta (IL-1β), and reactive oxygen species (Abbas et al., 2002; Janelsins et al., 2005; Wilkinson and Landreth, 2006). The chronic activation of the microglia compartment through continuous production of inflammatory mediators has been claimed as one of the principal causes that exacerbates neurodegeneration and thus the progression of AD (Glass et al., 2010; Schwab et al., 2010).

According to this scenario, great efforts have been committed to define the membrane microglia receptors that recognize the toxic amyloid species and that trigger signalling mechanisms responsible for the production of cytokines, aimed to design potential anti-inflammatory drugs in preventive treatments. Among these, a primary role has been assigned both to Toll-like receptors (TLR) and to Receptor for Advanced Glycation Endproducts (RAGE). In these studies, specific transcription factors for pro-inflammatory cytokines, as the NF-kB and

Abbreviations: ac-STAT3(K685), acetylated form of STAT3 on Lys685 residue; AD, Alzheimer's disease; APP, amyloid precursor protein; Aβ, amyloid beta peptides; CCL5, chemokine (C–C motif) ligand 5; JAKs, Janus kinases; p-STAT3(Y705), phosphorylated form of STAT3 on Tyr705 residue; RAGE, Receptor for Advanced Glycation End products; STAT3, Signal Transducers and Activators of Transcription protein 3; TLR, Toll-like receptors.

This paper is dedicated to the memory of our beloved colleague, Prof. Donatella Barra, for unforgettable guidance in science and life.

* Corresponding author. Dipartimento di Scienze Biochimiche, Sapienza, University of Rome, Piazzale Aldo Moro, 5, 00185 Roma, Italy. Tel.: +39 06 49910605; fax: +39 06 4440062.
E-mail address: eugenia.schinina@uniroma1.it (M.E. Schininà).

[1] These authors equally contributed to the work.

http://dx.doi.org/10.1016/j.neuint.2015.01.007
0197-0186/

AP1, have been pointed out in the amyloid-dependent phase of the microglia activation (Glass et al., 2010; Stewart et al., 2010).

Nevertheless, a notable work is still required to reveal the whole signalling landscape able to explain the transition of microglial cells towards the chronic production of inflammatory factors. In this regard, a challenge task is the discrimination at the molecular level between the events induced by the direct engagement by the amyloid oligomers of specific microglia receptors and the chronic production of inflammatory factors through autocrine/paracrine signalling. The Signal Transducers and Activators of Transcription proteins (STATs) are a family of latent cytoplasmic factors that, upon phosphorylation by components of Janus kinases family (JAKs) in response to the activation of membrane receptors by various cytokines and growth factors, form dimers that translocate in the nucleus, where they behave as transcriptional activators (Stark and Darnell, 2012). Different members of the STATs family are activated by distinctive cytokines. Phosphorylation of the Signal Transducers and Activators of Transcription proteins 3 (STAT3) is primarily induced by specific members of the interleukin family, including IL-6 and leukaemia inhibitory factor (LIF). Dimers made up by phosphorylated STAT3 may interact with recognition sites on promoters involved in transcription of genes related to cellular processes such as cell growth and apoptosis (Hutchins et al., 2013). The JAK/STAT3 system has been proven to be involved in the transcriptional regulation of many inflammatory factors (Cheon et al., 2011). Particularly, in the neuronal compartment the JAK/STAT3 signalling cooperates in the neurotoxicity induced by beta amyloid exposure in neurons (Chiba et al., 2009; Wan et al., 2010), and is engaged in the chronic microglia activation by several stimuli and in the responsiveness for the microglia compartment to beta amyloid peptides (Capiralla et al., 2012; Juknat et al., 2013; Przanowski et al., 2013; Xiong et al., 2014; Yang et al., 2010b; Zhanga et al., 2014). However, molecular and kinetic details of the STAT3 involvement in the microglia-mediated neuroinflammation are still scant. Moreover, it has been determined that STAT3 is subjected to site-specific phosphorylation, acetylation, methylation and ubiquitination. The actual arrangement of these PTMs along the STAT3 primary structure could be considered like a molecular code in addressing STAT3 isoforms to trigger diverse cellular events (Murase, 2013; Yang and Stark, 2008; Yang et al., 2010a; Zhuang, 2013), comprising the complex signalling leading to early and late responsiveness to amyloid.

Recently, we employed murine cells to monitor the effects of amyloid beta peptides in triggering the long-term microglial activation, at the proteome level (Di Francesco et al., 2012). Among a limited number of differentially expressed proteins, the 14-3-3 epsilon protein was found significantly up-regulated. 14-3-3 epsilon belongs to a regulatory protein family involved in important cellular processes (Lalle et al., 2013), including those leading to neurodegenerative diseases (Fujii et al., 2013; Sai et al., 2013). Since the 14-3-3 epsilon increased expression suggests a role of this protein in tuning microglia activation, the discovery of the signalling pathway responsible for the modulation of its expression level could be valuable for focusing strategies to lessen the inflammatory processes.

In this paper we aimed to go in details on the involvement and dynamics of alternative STAT3 isoforms in microglia challenged with the extracellular presence of Aβ peptides. We therefore investigated the early onset of a persistent activation of microglia by following expression of STAT3 isoforms and 14-3-3 epsilon protein by immunodetection. As the main cell model we preferred BV2 cells, a cell line derived from *raf/myc*-immortalized murine neonatal microglia, most frequently used in studies in which adequate amounts of protein extracts are required (Blasi et al., 1990; Henn et al., 2009). However, most of the critical results have been validated also in primary microglia cultures derived from postnatal rat cortex. Results confirm the involvement of the JAK/STAT3 in the molecular response of microglial cells in the proposed AD model, and highlight a peculiar time-dependent mode of appearance of differently post-translational modified STAT3 species.

2. Materials and methods

2.1. Chemicals and biologicals

Calcium chloride, potassium chloride, sodium phosphate dibasic and potassium phosphate monobasic were purchased from Merck KgaA (Darmstadt, Germany). Tris–HCl and dithiothreitol (DTT) were from Bio-Rad (Hercules, CA, USA). Sodium orthovanadate, phenylmethylsulphonylfluoride (PMSF), Tween-20, $CaCl_2$, $MgCl_2$, SDS, and thiourea were supplied by Sigma-Aldrich (St. Louis, MO, USA).

Foetal calf serum (FCS), penicillin, streptomycin and L-glutamine, JAK-2 protein tyrosine kinase inhibitor AG490, and isolectin B4 were purchased from Sigma-Aldrich. Synthetic $A\beta_{25-35}$ (GSNKGAIIGLM) and reverse $A\beta_{35-25}$ (MLGIIAGKNSG) were from Bachem (AG, Bubendorf, Switzerland). Dulbecco's modified Eagle's medium (DMEM) was supplied by Invitrogen Corporation (Carlsbad, CA, USA). Polyvinylidene difluoride (PVDF) Immobilon® membranes were from Millipore.

Sprague Dawley rats were from Charles River; BV2 cells is an immortalized cell line, continuously maintained at the Dipartimento di Scienze Anatomiche, Istologiche, Medico-Legali e dell'Apparato Locomotore, from an original gift of Prof. Giulio Levi (Istituto Superiore di Sanità, Rome).

2.2. Cell cultures

The murine microglial cell line BV2 (Blasi et al., 1990) was grown in Dulbecco's modified Eagle's medium (DMEM) supplemented with 10% (v/v) foetal calf serum (FCS), 100 units/mL penicillin, 100 μg/mL streptomycin and 2 mM L-glutamine; cultures were maintained at 37 °C in 5% CO_2/95% humidified air atmosphere.

Primary microglial cell cultures were derived from postnatal day 3–4 rat cortex as previously described (Novarino et al., 2004). Briefly, free-floating microglia were collected from shaken astrocyte flasks and maintained in DMEM supplemented with 10% (v/v) FCS in 5% CO_2.

2.3. Amyloid preparation

Synthetic $A\beta_{25-35}$ (GSNKGAIIGLM) and reverse $A\beta_{35-25}$ (MLGI IAGKNSG) peptides were dissolved in sterile, distilled water at a concentration of 1 mM, and preliminary incubated for 72 h at 37 °C to allow aggregation (Millucci et al., 2009).

2.4. Microglia cell treatments

Three replicates for each of resting, $A\beta_{25-35}$ and $A\beta_{35-25}$ treated BV2 cells were carried out. For this purpose, cells were cultured in 24-well culture plates (3×10^5 cells/well for primary microglia and 10^5 cells/well for BV2), washed with serum-free media, $A\beta_{25-35}$ or $A\beta_{35-25}$ peptides added to final concentrations of 25 μM for primary microglia and 50 μM for BV2, and cells challenged for 15 min, 30 min, 1 h, 4 h and 24 h.

In experiments aimed to assay the involvement of specific kinases, microglia activated by amyloid peptides were pre-treated with a solution of JAK-2 protein tyrosine kinase inhibitor AG490 (25 μM for primary microglia and 50 μM for BV2) for 18 h, then $A\beta_{25-35}$ peptide was added as described above.

In the experiments aimed to assay the involvement of the IL-6 signalling in the STAT3 activation, neutralization of the IL-6 activity was accomplished in BV2 cells by pre-treatment with 500 ng/mL of anti IL-6 antibody (Abcam; cat. n. ab6672) or control

nonspecific IgG for 24 h. Then, cells were treated with $A\beta_{25-35}$ as described above.

2.5. Immunocytochemistry

The purity of microglial cultures was >90%, as assessed by a positive immunostaining for *Griffonia simplicifolia* isolectin B4 and for OX-42. Microglial cell cultures contained <1% of astrocytes, as shown by glial fibrillar acidic protein (GFAP) immunostaining.

Morphological changes of primary microglial cell upon $A\beta_{25-35}$ or treatment with the JAK-2 protein tyrosine kinase inhibitor AG490 were followed by immunostaining for OX-42. Treated cells were washed and fixed in 4% (w/v) paraformaldehyde for 30 min. After saturation of non specific sites with 10% (v/v) normal donkey serum and 0.1% (w/v) Triton X-100 in phosphate buffered saline (PBS), cells were incubated with mouse anti-OX-42 antibody (Serotec MCA275G, Oxford, UK; antibody dilution 1:50) for 1 h at room temperature and, after washings, with a donkey Cy3-labelled anti-mouse IgG (Jackson ImmunoResearch Laboratories; antibody dilution 1:400). Negative controls were performed substituting specific IgGs with an equivalent amount of nonspecific IgG. Coverslips were mounted with Vectashield mounting medium containing 4′,6-diamidino-2-phenylindole (DAPI) for nuclear staining (Vector Laboratories, Burlingame, CA). Examinations and photographs were made using a fluorescent microscope (Eclipse E600; Nikon Instruments S.p.A., Firenze, Italy).

2.6. Cell viability

Viability in the presence of AG490 was assessed on BV2 by the MTT assay. Briefly, cells (1×10^4) were incubated in triplicate in a 96-well plate in the presence or absence of 50 μM AG490 for 18 h, then 50 μM $A\beta_{25-35}$ was added for 1 h, 4 h and 24 h at 37 °C. Thereafter, 100 μL of MTT solution (12 mM in PBS) was added to each well and after 3 h of incubation at 37 °C, water-insoluble dark blue formazan crystals that formed from the MTT cleavage in actively metabolizing cells were dissolved in DMSO. Optical densities were measured at 570 nm using a scanning multi-well spectrophotometer (Appliskan).

2.7. Western blot analyses

At the end of each incubation time, cells were harvested, washed twice with a phosphate saline buffer (PBS) containing 1.37 M NaCl, 27 mM KCl, 100 mM Na_2HPO_4, 18 mM KH_2PO_4, and lysed in 70 μL of a buffer containing 20 mM Tris–HCl pH 8.00, 2% (w/v) SDS, 100 mM thiourea, 40 mM dithiothreitol (DTT), 2 mM Na_3VO_4, 0.25 mM phenylmethylsulphonylfluoride (PMSF). After sonication (30 s, 8 times) samples were boiled at 95 °C for 5 min and then centrifuged for 30 min at 20,000 *g* at 4 °C. Protein extracts were resolved by 10% (w/v) sodium dodecyl sulphate (SDS)-polyacrylamide gel electrophoresis (SDS-PAGE; 200 V, 45 min). Protein bands were electrotransferred to polyvinylidene difluoride (PVDF) membranes (80 mA, 45 min). Membranes were then treated with 5% (w/v) ECL blocking agent (GE Healthcare Bio-Sciences) in a denaturating saline buffer (T-TBS) containing 0.1% (w/v) Tween-20, 10 mM Tris–HCl, 150 mM NaCl, 1 mM $CaCl_2$, and 1 mM $MgCl_2$, pH 7.4, for 1 h and then incubated with primary antibody overnight at 4 °C. Subsequently, membranes were washed three times in T-TBS, and bound antibodies were detected using appropriate horseradish peroxidase-conjugated secondary antibodies, followed by an ECL Plus Western blotting Detection System (GE Healthcare Bio-Sciences). ECL was detected using a Molecular Imager® ChemiDoc™ mod. MP System (Bio-Rad Laboratories), acquired by ImageLab Software ver. 4.1, and quantified using ImageJ analysis software (http://rsbweb.nih.gov/ij/). Analyses were performed in triplicate. Immunodetections were carried out using polyclonal antibodies (Cell Signaling Technology; antibody dilution 1:1000) against STAT3 (cat. n. 9132), STAT3 phosphorylated species at Tyr705 (cat. n. 9131) and Ser727 (cat. n. 9134) residues, STAT3 acetylated species at Lys685 (cat. n. 2523), 14-3-3 epsilon and GAPDH (Santa Cruz Biotechnology, sc-1020 and sc-32233, respectively; antibody dilution 1:500). In each analysed sample, signal of the target protein was normalized to the corresponding GAPDH level. At least three experimental replicates were performed for each biological sample. All results are expressed as mean ± SD. Differences between experimental groups were determined by Student's t-test. *p*-value of <0.01 was considered statistically significant.

2.8. Total RNA preparation and real-time PCR

Total RNA was isolated from BV2 cells after different treatments with TRIzol® (Invitrogen AG) following the manufacturer's instructions. The levels of mRNA were quantified by NanoDrop 1000 Spectrophotometer (Thermo Fisher Scientific). The first-strand complementary DNAs were generated with cDNA Synthesis Kit (Bioline). Real-time PCR amplification of cDNA was performed using the SYBER Green fluorophore by means of Brilliant® SYBER® Green qPCR Master Mix (Stratagene) in a MJ MiniOpticon Detection System (Bio-Rad Laboratories). Conditions for cDNA amplifications were as follows: 30 s at 95 °C, 30 s at 58 °C, 30 s at 72 °C, 40 cycles. The measurements were repeated at least three times. GAPDH cDNA was used as reference for normalization and the relative quantification was analysed using Gene Expression analysis for iCycler iQ real-time PCR detection system software, Version 1.10 (Bio-Rad Laboratories).

The primer sequences of each gene were as follows: GAPDH sense primer: 5′-CCTTCCGTGTTCCTACCC, antisense primer: 5′-AAGTCGC AGGAGACAACC; CCL5 sense primer: 5′-TGCCCACGTCAAGGAGTATTT; antisense primer: 5′-TCTCTGGGTTGGCACACACTT.

2.9. Bioinformatics

Promoter analyses were performed by the Genomatix Software Suite package at http://www.genomatix.de. Promoter structural details were automatically retrieved from genomic annotation deposited in Genomatix databases with the ElDorado program. Automatic searching for transcription factor binding site was performed with the MatInspector program.

3. Results

Primary and immortalized microglia cell cultures were challenged with $A\beta_{25-35}$ peptide, the neurotoxic domain of the full-length $A\beta_{1-42}$ peptide (Varadarajan et al., 2001). Both $A\beta_{1-42}$ and $A\beta_{25-35}$ have been demonstrated to induce toxic and oxidative effects on neuronal cells, with overlapping results (Varadarajan et al., 2001). The shorter form $A\beta_{25-35}$ has been frequently used in investigations of Aβ properties because it is a more manageable substitute than the native full-length peptide, ensuring reliable and reproducible results (Ghasemi et al., 2014; Khan et al., 2014; Martire et al., 2013; Sonkar et al., 2014). Aggregation studies in H_2O (Millucci et al., 2009) showed that the peptide $A\beta_{25-35}$ is prone to aggregate in a very short time after dissolution, also at low temperature. However, to increase homogeneity of the aggregated molecular species, we followed a protocol already proven to attain a high reproducibility in the biological response of microglia to the amyloid peptide (Di Francesco et al., 2012; Novarino et al., 2004; Paradisi et al., 2008).

In Fig. 1, immunostaining of primary microglia cells for the specific marker OX-42 is reported at resting and in the $A\beta_{25-35}$ activated status. Even if microglia morphology alone cannot be considered a univocal indicator of a specific functional stage (Colton and Wilcock,

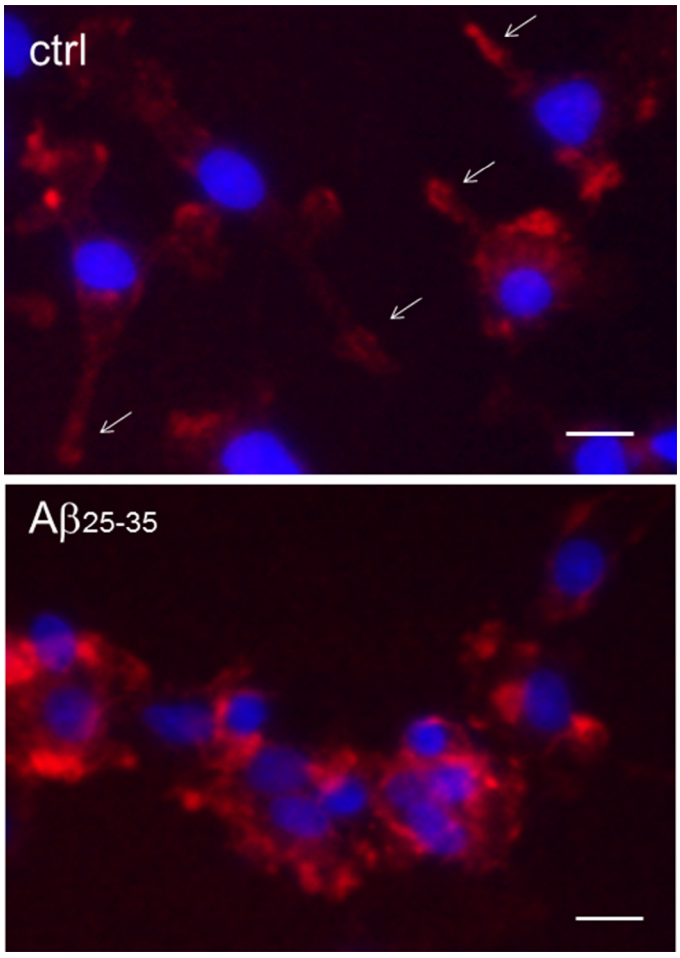

Fig. 1. Microglia morphological changes associated to amyloid beta peptide treatment. Primary microglial cells were activated by treatment with 25 μM $A\beta_{25-35}$ for 24 h (lower panel, $+A\beta_{25-35}$) or left untreated (upper panel, ctrl). Fluorescent microscopic analysis of resting and amyloid activated microglia by immunostaining for the microglial marker OX-42. While many processes (arrows) are observed in untreated control microglia, $A\beta_{25-35}$ treated cells appear round and clustered. Nuclei were counterstained with DAPI. Scale bar 5 μm.

2010), after $A\beta_{25-35}$ treatment microglial cells are clustered and round with few processes which conversely appear more numerous in untreated cells.

Firstly, we monitored the STAT3 expression changes in murine microglial cell cultures in the absence and in the presence of $A\beta_{25-35}$ amyloid species. To highlight possible transient changes in the protein level, data were collected on primary and immortalized cells at five stimulation times (15 min, 30 min, 1 h, 4 h and 24 h), thus encompassing both earlier and later events in the microglia activation. Results in Fig. 2, showed that expression levels of STAT3 remained stable up to 24 h from stimulation, and at comparable level between treated and untreated microglial cells. This indicates that amyloid does not evoke an increase of the transcriptional rate of the STAT3 gene at any of the analysed times. Since the shifting of STAT3 from a cytoplasmic latent form to signal transducer and transcriptional activator primarily resides on phosphorylation of the Tyr705 residue (Aggarwal et al., 2009), in the same experiments we measured the cell abundance of this specific phosphorylated species of STAT3, herein named p-STAT3(Y705). As evident from Fig. 2A, the p-STAT3(Y705) showed a drastic increase at 4 h in stimulated BV2, coming back to the basal value at 24 h. The presence of an alternative phosphorylation on Ser727 has been excluded using appropriate antibodies (Fig. 2A). The same results were obtained when primary microglial cells were challenged with the $A\beta_{25-35}$ peptide (Fig. 2B), confirming a similar behaviour of primary and immortalized cells.

Similar experimental setup was applied to monitor STAT3 acetylation at Lys685, herein named ac-STAT3(K685). In both BV2 and primary microglia cultures, an increase of the ac-STAT3(K685) took place at 1 h after stimulation, coming back to the basal levels at 4 h (Fig. 3). Thus in amyloid activated microglia, we observed that phosphorylation and acetylation occur in an unrelated mode, with acetylated and phosphorylated species accumulating at distinct times.

Treatments of microglia cells with the reverse $A\beta_{35-25}$ peptide failed to induce STAT3 changes demonstrating that only the amyloidogenic peptide $A\beta_{25-35}$ was able to trigger the STAT3 acetylation and phosphorylation (Supplementary Fig. S1).

With the aim of monitoring the involvement of JAKs in the post-translational modification of STAT3, the same experiments reported above were carried out in the presence of AG490, a specific inhibitor of this kinase family (Meydan et al., 1996), that did not alter the morphological transition induced by the $A\beta_{25-35}$ in the primary microglia cells as well as BV2 viability (Supplementary Fig. S2). In the presence of the JAK inhibitor, the increase of p-STAT3(Y705) detectable after 4 h stimulation was missed. On the contrary, this inhibitor induced neither changes of STAT3 levels nor affected the ac-STAT3(K685) expression level, indicating that the acetylation of STAT3 observed at 1 h was not dependent on the JAK signalling (Fig. 4).

Finally, we embarked on the demonstration of the transcriptional activity of the JAK/STAT3 pathway, monitoring the expression levels of the (CC) chemokine 5 (CCL5), known to be specifically under the STAT3 transcriptional control (Przanowski et al., 2013). By RT-PCR we measured the transcriptional levels of *ccl5* after 1, 4 and 24 h during amyloid stimulation, observing at 24 h the highest level of gene expression. As expected, transcription of the mRNA for this chemokine measured by specific primers (Supplementary Fig. S3) was inhibited by the presence of the JAK inhibitor AG490, confirming that the JAK/STAT3 pathway is responsible of this delayed inflammatory response of activated microglia (Fig. 5). It is not easy to explain why in the presence of inhibitor AG490 the *ccl5* expression dropped at 24 h under basal levels.

The protein 14-3-3 epsilon is a member of the 14-3-3 protein family, known to interact with phosphorylated proteins, and to modulate the signal transduction pathways behaving as a scaffold agent (Obsil and Obsilova, 2011). Our previous proteomic studies showed that 14-3-3 epsilon specifically marks the activation of microglia triggered by $A\beta_{25-35}$ (Di Francesco et al., 2012). Bioinformatics analysis of the 14-3-3 epsilon gene promoter highlighted one putative STAT3 recognition site (http://www.genomatix.de; Fig. 6A). Accordingly, in this work, we investigated if beta amyloid was able to increase microglia 14-3-3 epsilon levels through the activation of the JAK/STAT3 pathways. As evident from Fig. 6, in amyloid-activated BV2 (panel B) and primary microglia cells (panel C) 14-3-3 epsilon increases in expression at 24 h, reproducing our previous result. The involvement of p-STAT3(Y705) in the increased expression of 14-3-3 epsilon was confirmed after treatment with the JAK inhibitor AG490. It is noteworthy that even the 14-3-3 epsilon expression dropped at 24 h under basal levels in the presence of inhibitor AG490, as observed for CCL5.

Aimed to assess if the observed STAT3 phosphorylation is delayed in consequence of the temporal gap required for cytokine production triggered by the direct beta amyloid stimulation, we activated cells with the amyloid peptide upon neutralization of the IL-6 signalling. Indeed, as evident in Fig. 7, in BV2 treated with $A\beta_{25-35}$ the presence of antibodies against IL-6 did inhibit STAT3 phosphorylation without affecting its acetylation. Moreover, also the overexpression of 14-3-3 epsilon was suppressed.

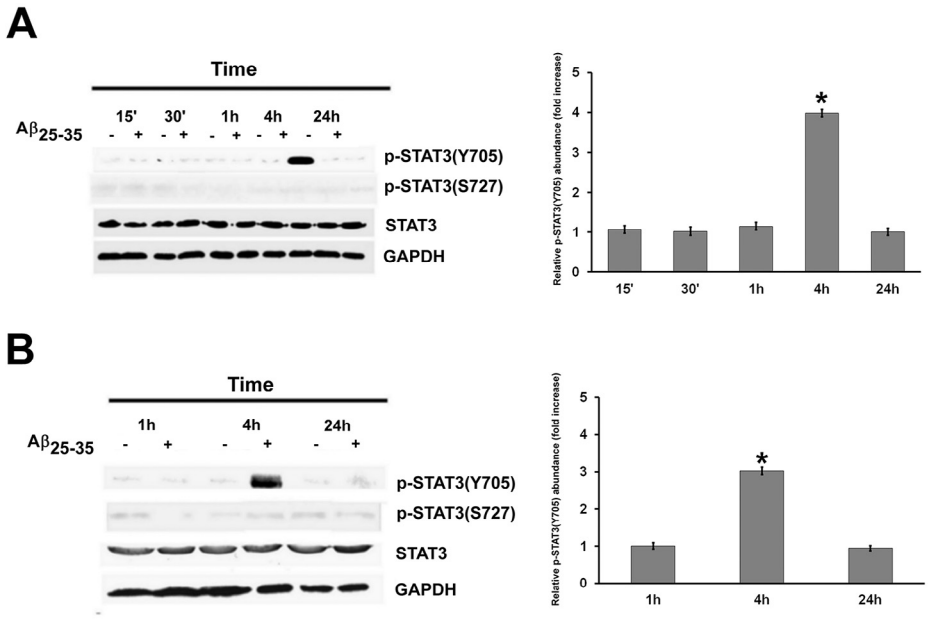

Fig. 2. Effects of amyloid beta peptide on the relative abundance of phosphorylated species of STAT3 in microglial cells. Relative abundance of p-STAT3(Y705), p-STAT3(S727) and STAT3 in BV2 (A) and in primary microglia (B) cells is reported. On the left, representative immunoblots for p-STAT3(Y705), p-STAT3(S727) and total STAT3 at different time intervals are shown. $A\beta_{25-35}$ was added to final concentrations of 25 μM for primary microglia and 50 μM for BV2. $A\beta_{25-35}$ treated (+) and untreated (−) cells. On the right, quantification of p-STAT3(Y705) is reported. Fold increase values represent the ratio between optical densities of p-STAT3(Y705) in treated and untreated microglia cells, both normalized to the corresponding GAPDH bands. Quantitative data were collected from three independent cell preparations, from which three western blot replica were carried out (n = 3) and averaged (±SD). Statistical analysis was performed by T-student test; $^{*}p < 0.01$ *vs* control BV2 (A) and control primary microglia cells (B).

4. Discussion

Nowadays, inflammatory processes are considered a critical part in the progression of chronic pathologies. In agreement with this updated viewpoint, efforts in the studies on neurodegenerative diseases are dedicated to correlate microglia activation with neurotoxic processes.

Many pro-inflammatory factors produced by activated microglia have been indicated as responsible for the interplay between these sentinel cells and neurons. These cytokines (*i.e.* TNF-alpha, IL-6 and IL-1β) are released as a direct consequence of activation of receptors on the microglia membrane (Glass et al., 2010).

In Alzheimer's disease models, evidence has been reported for TLR and RAGE as the receptors stimulated by extracellular

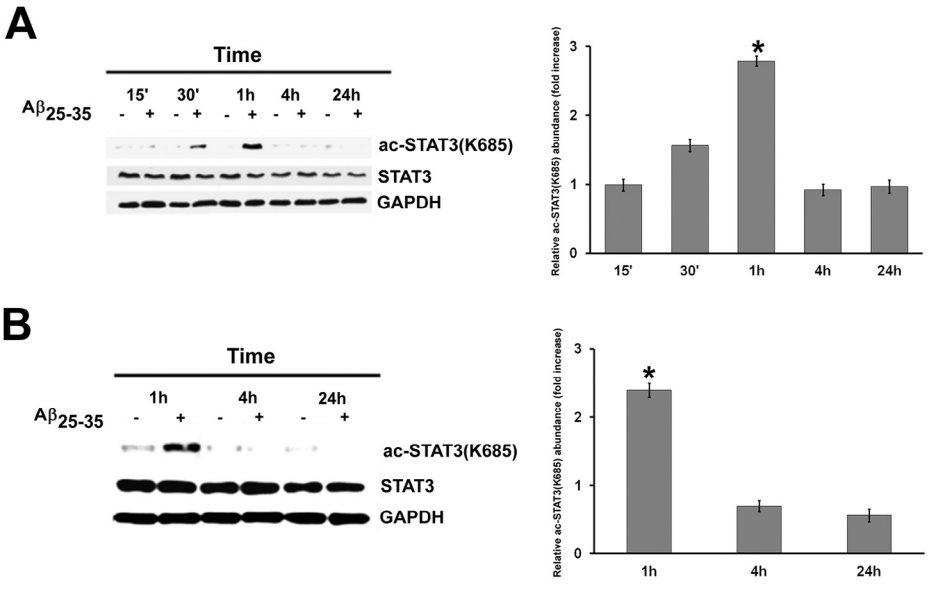

Fig. 3. Effects of amyloid beta peptide on the relative abundance of acetylated species of STAT3 in microglial cells. Relative abundance of ac-STAT3(K685) in BV2 cells (A) and in primary microglia cells (B) is reported. On the left, representative immunoblots for ac-STAT3(K685) and total STAT3 at different time intervals are shown. $A\beta_{25-35}$ was added to final concentrations of 25 μM for primary microglia and 50 μM for BV2; $A\beta_{25-35}$ treated (+) and untreated (−) cells. On the right, quantification of ac-STAT3(K685) is reported. Fold increase values represent the ratio between the optical densities of ac-STAT3(K685) in treated and untreated microglia cells, both normalized to the corresponding GAPDH bands. Quantitative data were collected from three independent cell preparations, from which three western blot replica were carried out (n = 3), and averaged (±SD). Statistical analysis was performed by T-student test; $^{*}p < 0.01$ *vs* control BV2 (A) and control primary microglia cells (B).

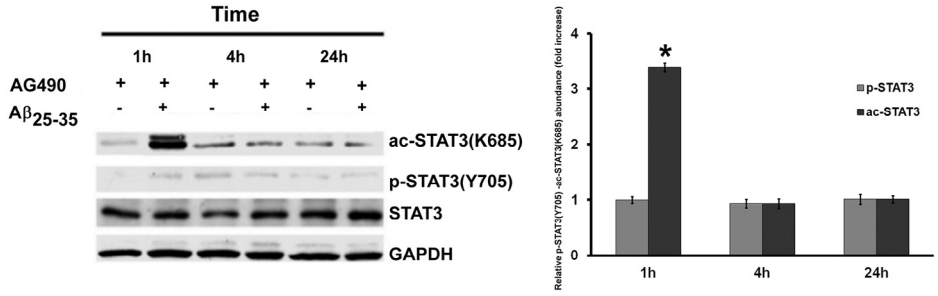

Fig. 4. Effects of the JAKs inhibition on the relative abundance of ac-STAT3(K685) and p-STAT3(Y705) species. On the left, representative immunoblots for ac-STAT3(K685), p-STAT3(Y705) and total STAT3 are shown. BV2 cells were incubated with a 50 μM AG490 (+) for 18 h alone (–) or in combination with 50 μM $A\beta_{25-35}$ (+). Refer to Fig. 2 and Fig. 3 for the BV2 sample treated with $A\beta_{25-35}$ in the absence of the inhibitor. Quantification of ac-STAT3(K685) and p-STAT3(Y705) is reported on the right. Fold increase values represent the ratio between the optical densities of each of these species in treated and untreated BV2 cells, normalized to the value of the corresponding GAPDH band. Quantitative data were collected from three independent cell preparations, from which three western blot replica were carried out (n = 3), and averaged (±SD). Statistical analysis was performed by T-student test; *$p < 0.01$ *vs* BV2 cells treated with AG490 alone.

amyloidogenic peptides in microglia cultures. These amyloid activated receptors trigger the activation of NF-kB and AP-1 responsive machineries for the release of specific cytokines. This process may be considered as an early molecular event in microglia activation directly evoked by the amyloidogenic molecules (Glass et al., 2010).

JAK/STAT signalling is an important signalling pathway widely involved in chronic diseases, and studies on its involvement in neurodegenerative diseases, and in particular in microglia, are in rapid progress (Capiralla et al., 2012; Juknat et al., 2013; Przanowski et al., 2013; Xiong et al., 2014; Yang et al., 2010b; Zhanga et al., 2014). In this work, our principal purpose was to determine kinetics details of the involvement of different isoforms of STAT3, a well known mediator involved in chronic diseases, in the responsiveness of microglia to amyloidogenic peptides.

Thanks to our experimental setup, in which microglia responsiveness to amyloid peptides was monitored up to 24 h, we observed that p-STAT3(Y705) is detectable in our cell models only at 4 h, as results of JAK activation. Since this JAK/STAT3 activation is widely delayed with respect to the early release of cytokines in response to the amyloid exposure, it is reasonable that STAT3 activation is not directly triggered by the stimulation of membrane receptors by amyloid. We explained this delayed expression of p-STAT3(Y705) in terms of release of IL-6, one of the cytokines known to be released in the early phase following inflammatory activation of microglia by amyloid (Hirano et al., 2000; Kumar and Ward, 2014). According to these results, the following cascade of events is reasonable to occur: i) amyloid oligomers engage specific receptors; ii) activation of these receptors induces the expression and the release of specific cytokines; iii) among these, IL-6 is able, in an autocrine/paracrine manner, to stimulate the JAK/STAT3 systems. This sequential signalling network we suggest for microglia responsiveness to beta amyloid supports a similar model recently proposed by the Kamiska's group for the responsiveness of the same cells to LPS stimulation (Przanowski et al., 2013).

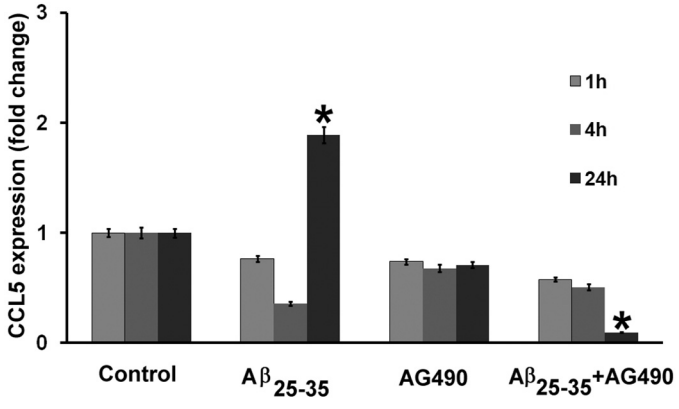

Fig. 5. Expression of *ccl5* gene in BV2 cells stimulated by $A\beta_{25-35}$. The mRNA expression is compared among untreated BV2 resting cells (control), 50 μM amyloid peptide treated cells ($A\beta_{25-35}$), cells treated with 50 μM solution of the JAK inhibitor AG490 (AG490), and cell pre-treated with 50 μM AG490 and then stimulated with 50 μM $A\beta_{25-35}$ (AG490 + $A\beta_{25-35}$). The expression level of the gene is reported as fold change relative to the control, normalized to the level of GAPDH cDNA as housekeeping gene. Values were determined at 1 h, 4 h and 24 h. All bars represent mean ± SD. Statistical analysis was performed by T-student test; *$p < 0.01$ *vs* control BV2 cells.

Recently, we investigated the differentially expression pattern in amyloid activated microglia by proteomics (Di Francesco et al., 2012). The expression changes we reported established 14-3-3 epsilon as a marker of the events occurring in the proteome of microglia activated by amyloid, where it may act as a crucial modulator of the complex signals triggered by amyloid through its intrinsic promiscuity towards phosphorylated proteins. In the 14-3-3 epsilon promoter we identified one putative STAT3 binding site. According to the results here reported, the expression of 14-3-3 epsilon actually appears to be under the JAK/STAT3 control. The full understanding of the molecular events that arise from the STAT3-dependent 14-3-3 epsilon expression requires further investigations.

Beside phosphorylation, other post-translational modifications have been proven to be encompassed in the molecular barcode for the transcriptional activity of STAT3 (Stark and Darnell, 2012). Among these, acetylation has been reported to be involved in diverse functional roles of STAT3 (Zhuang, 2013). Particularly, a critical role in the stabilization of STAT3 homodimers has been reported for acetylation of Lys685 by the mammalian histone acetyltransferase complex CBP/p300 (Wang et al., 2005; Yuan et al., 2005). Our results showed for the first time that in the amyloid activated microglia the abundance of ac-STAT3(K685) species increased at an early time (1 h), but at 4 h, when p-STAT3(Y705) accumulated, the level of the acetylated species was observed to be the basal levels. The changes in STAT3 acetylation we observed were independent from the JAK activation and overall these results suggest that in our system acetylation does not cooperate with phosphorylation in the transcriptional activity of STAT3.

The microglia responsiveness to Aβ peptides thus seem to rely on diverse post-translational modifications of the transcriptional activator STAT3, through a commitment distinguishable in at least two-phases: the acetyl code that synchronizes with the first reaction of microglia to amyloid, and the phosphoryl code appearing in a delayed time.

In the neuronal compartment activation of STAT3 has been observed in the presence of beta amyloid (Wan et al., 2010), and it is

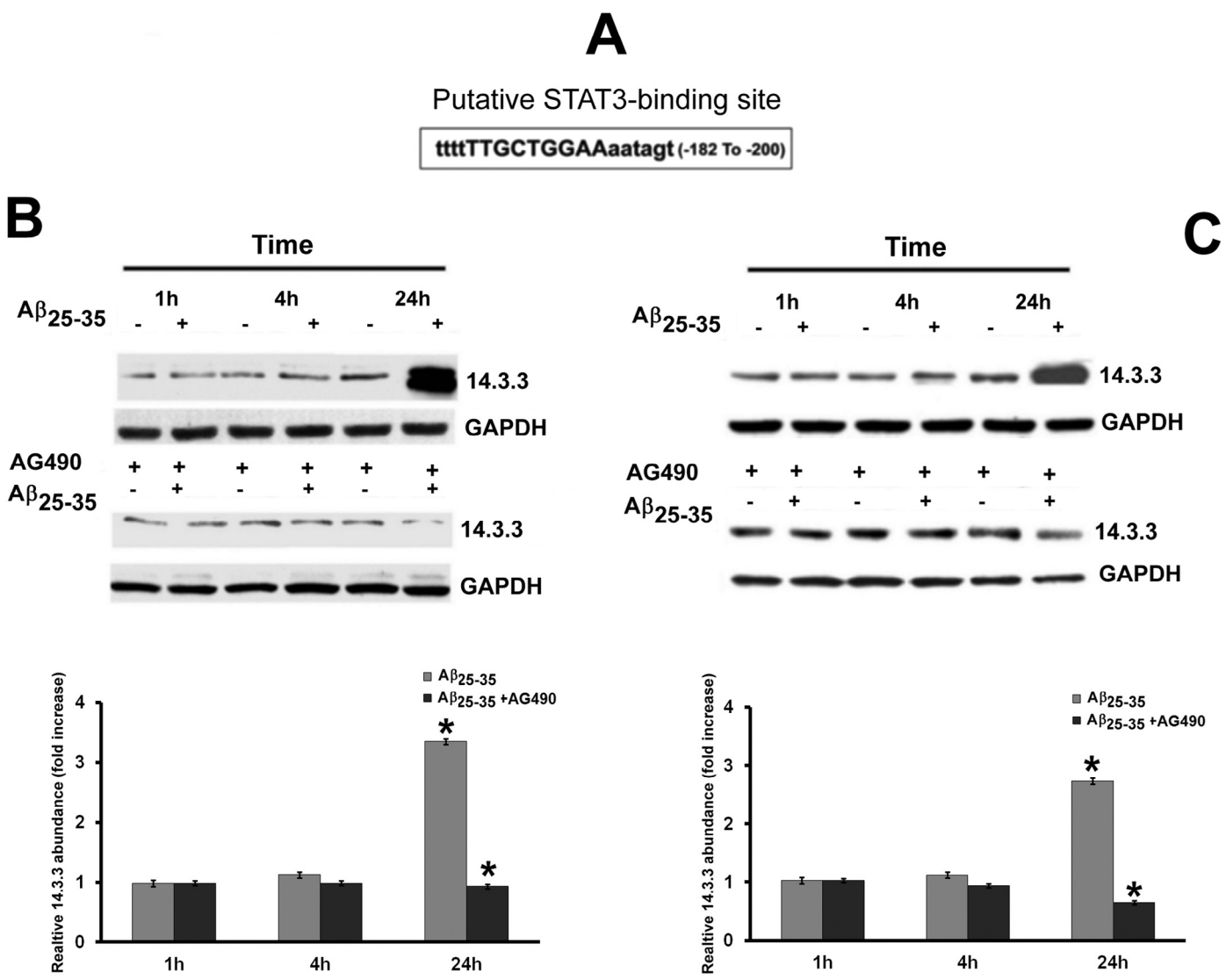

Fig. 6. Expression of 14-3-3 epsilon depending on the JAK/STAT3 signalling. Putative binding site in the 14-3-3 epsilon promoter is shown in (A). Relative abundance of 14-3-3 epsilon in BV2 cells (B) and in primary microglia cells (C) is reported. In the upper section of (B) and (C), representative immunoblots for 14-3-3 epsilon protein are shown. Results from cell untreated ($A\beta_{25-35}$–) or treated ($A\beta_{25-35}$+) with the amyloid peptide (upper immunoblots) have been compared with that obtained from cells pre-incubated with a 50 μM solution of the inhibitor ($A\beta_{25-35}$–/AG490 + and $A\beta_{25-35}$ +/AG490+; lower immunoblots). Quantification of relative abundance of 14-3-3 epsilon protein is reported (lower sections). Fold increase values represent the ratio between the optical densities of 14-3-3 epsilon protein in AG490 treated and untreated BV2 and primary cells, normalized to the value of the corresponding GAPDH band. Quantitative data were collected from three independent cell preparations, from which three western blot replica were carried out (n = 3), and averaged (±SD). Statistical analysis of the 14-3-3 epsilon protein expression in presence and in absence of AG490 was performed by T-student test; $^{*}p < 0.01$ *vs* control BV2 and primary cells.

involved in the neuronal loss by apoptosis that marks AD. Conversely, since in microglia the presence of beta amyloids is well known to induce cell proliferation, STAT3 is unlike to be an apoptosis-inducer in this compartment. Thus this work seems to outline diverse but complementary roles of STAT3 signalling, *i.e.* triggering neuronal apoptosis (Wan et al., 2010) and microglia activation, both causing synergic effects for the AD progression.

5. Conclusions

Our results highlighted three crucial timings in the involvement of the transcriptional modulator STAT3 in the microglia activation by Aβ amyloid: i) an early event, marked by increased level of the acetylated form of STAT3 in Lys685 with still unknown functional role; ii) a delayed event in which it predominates its isoform phosphorylated on Tyr705 residue, under the control of the released cytokine IL-6; and iii) a changing in cellular proteome towards a microglia chronically activated, marked by the increase of the 14-3-3 epsilon levels. These events outline a complex protein network triggered by amyloid in the microglial compartment. Further details of the dynamics of the amyloid trigged signalling will be crucial in broadening our understanding of the molecular basis of neurotoxicity.

Acknowledgements

This work has been partly supported by an Italian grant from MIUR (to MES; grant number PRIN 2010HEBBB8_002), by a Sapienza University grant (to MES; grant number C26A124WCR), by Istituto Pasteur-Fondazione Cenci Bolognetti and Credito Cooperativo Cassa Rurale ed Artigiana di Paliano (to ME). The funders had no role in study design, data collection and analysis, decision to publish, or

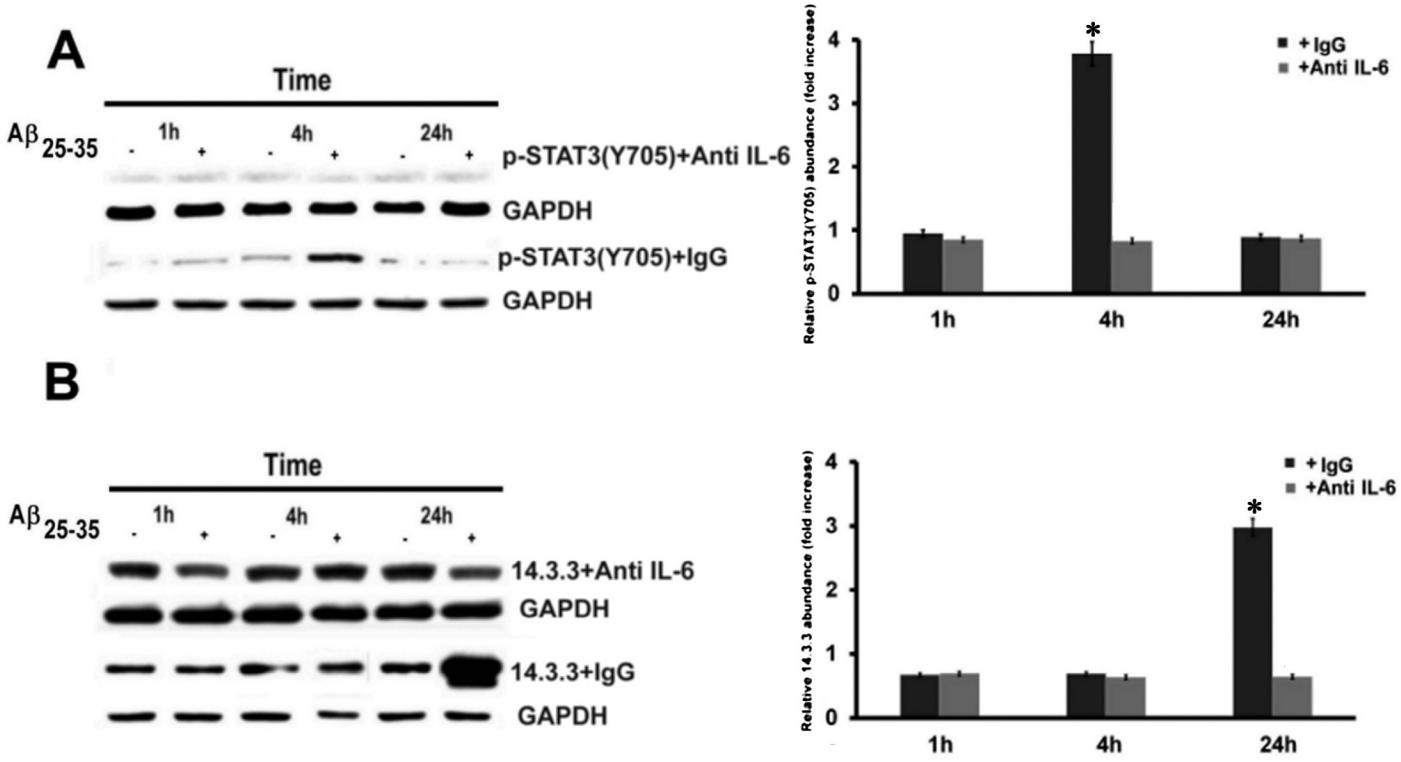

Fig. 7. Effects of the neutralization of IL-6 activity on the STAT3 phosphorylation and 14-3-3 epsilon expression. On the left, representative immunoblots for p-STAT3(Y705) (A) and 14-3-3 epsilon protein (B) in BV2 cells are shown, in the presence of antibodies against IL-6 (+anti IL-6). Control experiments were also performed (+IgG). $A\beta_{25-35}$ treated (+) and untreated (–) cells. On the right, quantification of p-STAT3(Y705) (A) and 14-3-3 protein (B) is reported. Fold increase values represent the ratio between optical densities of p-STAT3(Y705) and 14-3-3 protein in treated and untreated microglia cells, both normalized to the corresponding GAPDH bands. Quantitative data were collected from three independent cell preparations, from which three western blot replica were carried out (n = 3) and averaged (±SD). Statistical analysis was performed by T-student test; $^{*}p < 0.01$ *vs* control BV2 cells.

preparation of the manuscript. None of the authors have competing interests to declare.

Appendix: Supplementary material

Supplementary data to this article can be found online at doi:10.1016/j.neuint.2015.01.007.

References

Abbas, N., Bednar, I., Mix, E., Marie, S., Paterson, D., Ljungberg, A., et al., 2002. Up-regulation of the inflammatory cytokines IFN-γ and IL-12 and down-regulation of IL-4 in cerebral cortex regions of APPSWE transgenic mice. J. Neuroimmunol. 126, 50–57.

Aggarwal, B.B., Kunnumakkara, A.B., Harikumar, K.B., Gupta, S.R., Tharakan, S.T., Koca, C., et al., 2009. Signal transducer and activator of transcription-3, inflammation, and cancer: how intimate is the relationship? Ann. N. Y. Acad. Sci. 1171, 59–76.

Ballard, C., Gautheier, S., Corbett, A., Brayne, C., Aarsland, D., Jones, E., 2011. Alzheimer's disease. Lancet 377, 1019–1031.

Birch, A.M., Katsouri, L., Sastre, M., 2014. Modulation of inflammation in transgenic models of Alzheimer's disease. J. Neuroinflammation 11, 25.

Blasi, E., Barluzzi, R., Bocchini, V., Mazzolla, R., Bistoni, F., 1990. Immortalization of murine microglial cells by a v-raf/v-myc carrying retrovirus. J. Neuroimmunol. 27, 229–237.

Blennow, K., de Leon, M.J., Zetterberg, H., 2006. Alzheimer's disease. Lancet 368, 387–403.

Capiralla, H., Vingtdeux, V., Zhao, H., Sankowski, R., Al-Abed, Y., Davies, P., et al., 2012. Resveratrol mitigates lipopolysaccharide- and Aβ-mediated microglial inflammation by inhibiting the TLR4/NF-κB/STAT signaling cascade. J. Neurochem. 120, 461–472.

Cheon, H., Yang, J., Stark, G.R., 2011. The functions of signal transducers and activators of transcriptions 1 and 3 as cytokine-inducible proteins. J. Interferon Cytokine Res. 31, 33–40.

Chiba, T., Yamada, M., Sasabe, J., Terashita, K., Shimoda, M., Matsuoka, M., et al., 2009. Amyloid-ß causes memory impairment by disturbing the JAK2/STAT3 axis in hippocampal neurons. Mol. Psychiatry 14, 206–222.

Colton, C.A., Wilcock, D.M., 2010. Assessing activation states in microglia. CNS Neurological. Disord. Drug Targets 9, 174–191.

Cunningham, C., 2013. Microglia and neurodegeneration, the role of systemic inflammation. Glia 61, 71–90.

Di Francesco, L., Correani, V., Fabrizi, C., Fumagalli, L., Mazzanti, M., Maras, B., et al., 2012. 14-3-3ε marks the amyloid-stimulated microglia long-term activation. Proteomics 12, 124–134.

Fujii, K., Uchikawa, H., Tanabe, Y., Omata, T., Nonaka, I., Kohno, Y., 2013. 14-3-3 proteins, particularly of the epsilon isoform, are detectable in cerebrospinal fluids of cerebellar diseases in children. Brain Dev. 35, 555–560.

Ghasemi, R., Zarifkar, A., Rastegar, K., Maghsoudi, N., Moosavi, M., 2014. Repeated intra-hippocampal injection of beta-amyloid 25–35 induces a reproducible impairment of learning and memory: considering caspase-3 and MAPKs activity. Eur. J. Pharmacol. 726C, 33–40.

Glass, C.K., Saijo, K., Winner, B., Marchetto, M.C., Gage, F.H., 2010. Mechanisms underlying inflammation in neurodegeneration. Cell 140, 918–934.

Henn, A., Lund, S., Hedtjärn, M., Schrattenholz, A., Pörzgen, P., Leist, M., 2009. The suitability of BV2 cells as alternative model system for primary microglia cultures or for animal experiments examining brain inflammation. ALTEX 26, 83–94.

Herber, D.L., Mercer, M., Roth, L.M., Symmonds, K., Maloney, J., Wilson, N., et al., 2007. Microglial activation is required for Abeta clearance after intracranial injection of lipopolysaccharide in APP transgenic mice. J. Neuroimmune Pharmacol. 2, 222–231.

Hirano, T., Ishihara, K., Hibi, M., 2000. Roles of STAT3 in mediating the cell growth, differentiation and survival signals relayed through the IL-6 family of cytokine receptors. Oncogene 19, 2548–2556.

Hutchins, A.P., Diez, D., Takahashi, Y., Ahmad, S., Jauch, R., Tremblay, M.L., et al., 2013. Distinct transcriptional regulatory modules underlie STAT3's cell type-independent and cell type-specific functions. Nucleic Acids Res. 41, 2155–2170.

Janelsins, M.C., Mastrangelo, M.A., Oddo, S., LaFerla, F.M., Federoff, H.J., Bowers, W.J., 2005. Early correlation of microglial activation with enhanced tumor necrosis factor-alpha and monocyte chemoattractant protein-1 expression specifically within the entorhinal cortex of triple transgenic Alzheimer's disease mice. J. Neuroinflammation 2, 23.

Juknat, A., Pietr, M., Kozela, E., Rimmerman, N., Levy, R., Gao, F., et al., 2013. Microarray and pathway analysis reveal distinct mechanisms underlying cannabinoid-mediated modulation of LPS-induced activation of BV-2 microglial cells. PLoS ONE 8, e61462.

Khan, A., Vaibhav, K., Javed, H., Tabassum, R., Ahmed, M.E., Khan, M.M., et al., 2014. 1,8-cineole (eucalyptol) mitigates inflammation in amyloid Beta toxicated PC12 cells: relevance to Alzheimer's disease. Neurochem. Res. 39, 344–352.
Kumar, J., Ward, A.C., 2014. Role of the interleukin 6 receptor family in epithelial ovarian cancer and its clinical implications. Biochim. Biophys. Acta 1845, 117–125.
Lalle, M., Leptourgidou, F., Camerini, S., Pozio, E., Skoulakis, E.M., 2013. Interkingdom complementation reveals structural conservation and functional divergence of 14-3-3 proteins. PLoS ONE 8, e78090.
Martire, S., Fuso, A., Rotili, D., Tempera, I., Giordano, C., De Zottis, I., et al., 2013. PARP-1 modulates amyloid beta peptide-induced neuronal damage. PLoS ONE 8, e72169.
Mawuenyega, K.G., Sigurdson, W., Ovod, V., Munsell, L., Kasten, T., Morris, J.C., et al., 2010. Decreased clearance of CNS β-amyloid in Alzheimer's disease. Science 330, 1774.
Meydan, N., Grunberger, T., Dadi, H., Shahar, M., Arpaia, E., Lapidot, Z., et al., 1996. Inhibition of acute lymphoblastic leukaemia by a Jak-2 inhibitor. Nature 379, 645–648.
Millucci, L., Raggiaschi, R., Franceschini, D., Terstappen, G., Santucci, A., 2009. Rapid aggregation and assembly in aqueous solution of Aβ (25–35) peptide. J. Biosci. 34, 293–303.
Morkuniene, R., Zvirbliene, A., Dalgediene, I., Cizas, P., Jankeviciute, S., Baliutyte, G., et al., 2013. Antibodies bound to Aβ oligomers potentiate the neurotoxicity of Aβ by activating microglia. J. Neurochem. 126, 604–615.
Murase, S., 2013. Signal transducer and activator of transcription 3 (STAT3) degradation by proteasome controls a developmental switch in neurotrophin dependence. J. Biol. Chem. 288, 20151–20161.
Novarino, G., Fabrizi, C., Tonini, R., Denti, M.A., Malchiodi-Albedi, F., Lauro, G.M., et al., 2004. Involvement of the intracellular ion channel CLIC1 in microglia-mediated beta-amyloid-induced neurotoxicity. J. Neurosci. 24, 5322–5330.
Obsil, T., Obsilova, V., 2011. Structural basis of 14-3-3 protein functions. Semin. Cell Dev. Biol. 22, 663–672.
Paradisi, S., Matteucci, A., Fabrizi, C., Denti, M.A., Abeti, R., Breit, S.N., et al., 2008. Blockade of chloride intracellular ion channel 1 stimulates Abeta phagocytosis. J. Neurosci. Res. 86, 2488–2498.
Prokop, S., Miller, K.R., Heppner, F.L., 2013. Microglia actions in Alzheimer's disease. Acta Neuropathol. 126, 461–477.
Przanowski, P., Dabrowski, M., Ellert-Miklaszewska, A., Kloss, M., Mieczkowski, J., Kaza, B., et al., 2013. The signal transducers Stat1 and Stat3 and their novel target Jmjd3 drive the expression of inflammatory genes in microglia. J. Mol. Med. (Berl.) 92, 239–254.
Sai, Y., Peng, K., Ye, F., Zhao, X., Zhao, Y., Zou, Z., et al., 2013. 14-3-3 proteins in the regulation of rotenone-induced neurotoxicity might be via its isoform 14-3-3epsilon's involvement in autophagy. Cell. Mol. Neurobiol. 33, 1109–1121.
Schwab, C., Klegeris, A., McGeer, P.L., 2010. Inflammation in transgenic mouse models of neurodegenerative disorders. Biochim. Biophys. Acta 1802, 889–902.
Solito, E., Sastre, M., 2012. Microglia function in Alzheimer's disease. Front. Pharmacol. 3, 14.
Sonkar, V.K., Kulkarni, P.P., Dash, D., 2014. Amyloid β peptide stimulates platelet activation through RhoA-dependent modulation of actomyosin organization. FASEB J. 28, 1819–1829.
Stark, G.R., Darnell, J.E., Jr., 2012. The JAK-STAT pathway at twenty. Immunity 36, 503–514.
Stewart, C.R., Stuart, L.M., Wilkinson, K., van Gils, J.M., Deng, J., Halle, A., et al., 2010. CD36 ligands promote sterile inflammation through assembly of a Toll-like receptor 4 and 6 heterodimer. Nat. Immunol. 11, 155–161.
Thal, D.R., 2012. The role of astrocytes in amyloid β-protein toxicity and clearance. Exp. Neurol. 236, 1–5.
Varadarajan, S., Kanski, J., Aksenova, M., Lauderback, C., Butterfield, D.A., 2001. Different mechanisms of oxidative stress and neurotoxicity for Alzheimer's Aβ(1–42) and Aβ(25–35). J. Am. Chem. Soc. 123, 5625–5631.
Wan, J., Fu, A.K., Ip, F.C., Ng, H.K., Hugon, J., Page, G., et al., 2010. Tyk2/STAT3 signaling mediates beta-amyloid-induced neuronal cell death: implications in Alzheimer's disease. J. Neurosci. 30, 6873–6881.
Wang, R., Cherukuri, P., Luo, J., 2005. Activation of Stat3 sequence-specific DNA binding and transcription by p300/CREB-binding protein-mediated acetylation. J. Biol. Chem. 280, 11528–11534.
Wilkinson, B.L., Landreth, G.E., 2006. The microglial NADPH oxidase complex as a source of oxidative stress in Alzheimer's disease. J. Neuroinflammation 3, 30.
Xiong, J., Wang, C., Chen, H., Hu, Y., Tian, L., Pan, J., et al., 2014. Aβ-induced microglial cell activation is inhibited by baicalin through the JAK2/STAT3 signaling pathway. Int. J. Neurosci. 124, 609–620.
Yang, J., Stark, G.R., 2008. Roles of unphosphorylated STATs in signaling. Cell Res. 18, 443–451.
Yang, J., Huang, J., Dasgupta, M., Sears, N., Miyagi, M., Wang, B., et al., 2010a. Reversible methylation of promoter-bound STAT3 by hystone-modifying enzymes. Proc. Natl. Acad. Sci. U.S.A. 107, 21499–21504.
Yang, X., He, G., Hao, Y., Chen, C., Li, M., Wang, Y., et al., 2010b. The role of the JAK2-STAT3 pathway in pro-inflammatory responses of EMF-stimulated N9 microglial cells. J. Neuroinflammation 7, 54.
Yuan, Z.L., Guan, Y.J., Chatterjee, D., Chin, Y.E., 2005. Stat3 dimerization regulated by reversible acetylation of a single lysine residue. Science 307, 269–273.
Zhanga, Z., Yu, L., Hui, X., Wu, Z., Yin, K., Yang, H., et al., 2014. Hydroxy-safflor yellow A attenuates $A\beta_{1-42}$-induced inflammation by modulating the JAK2/STAT3/NF-κB pathway. Brain Res. 1563, 72–80.
Zhuang, S., 2013. Regulation of STAT signaling by acetylation. Cell. Signal. 25, 1924–1931.